Chapter 4

Chromium(III) Bidentate Phosphorus Chemistry

4.1 INTRODUCTION

The next class of compounds involved replacing the bidentate N–donor ligand, bipyridine, with a P–donor bidentate ligand, bis–diphenylphosphinoethane (dppe), while still maintaining the various substituted monodentate ligands as the secondary ligands.

The choice of dppe was based on the need to mimic the five–membered chelate ring that bipyridine formed when coordinated to the Cr(III) metal centre via substitution reactions of $[CrCl_3(thf)_3]$. The choice was also in keeping with known donor atoms that had been previously coordinated to Cr(III) to yield catalytically active species successfully [31].

Previously, Hermes and Girolami [112] synthesised the compound $[CrCl_3(dippe)(thf)]$, where dippe was diisopropylphosphinoethane. It was therefore of interest to exploit similar compounds with different steric and electronic properties as comparative studies could be undertaken. Also, by increasing the bulk of the ligand it was hoped to increase solubility and, in turn, increase the possibility of obtaining single crystals.

Furthermore, the addition of the substituted pyridines as secondary ligands had not been done previously.

Hermes and Girolami carried out ^1H NMR and IR analysis on their compound. However, the valuable IR data was not exploited in any detail and they simply documented a list of values with no band assignments. These values have, however, aided the detailed spectroscopic examination of the compounds of this study.

4.2 SYNTHESIS

Addition of one equivalent of dppe to an already dissolved one equivalent of $[CrCl_3(thf)_3]$ in thf afforded an immediate colour change from the characteristic deep precursor purple to a deep, dark blue. The reaction conditions of the previous classes were duplicated to ensure completion. As the substitution occurred so readily and remained in solution, the addition of the secondary pyridine ligands was straightforward. Unlike with the slowly coordinating bipyridine ligand, there was no concern about when to add the rapidly coordinating pyridine ligands so as to avoid them binding to all three of the metal sites before the bidentate dppe had done so. Upon the addition of the respective pyridine ligands, the solutions turned a notable blue-green colour which was perhaps expected as pyridine coordination to chromium results in an olive green-coloured reaction medium.

An interesting observation was the speed at which the addition of the dppe ligand to the chromium centre took place relative to its bipyridine counterpart. Although both appear to form stable five–membered chelate rings, the dppe coordinates immediately (formation of blue supernatant), while the bipyridine ligand, as previously discussed, only changes to its colour of coordination (green) and forms a precipitate after a fairly long period of time. The respective blue and green-coloured complexes were expected as they correlate well with the literature. It is simply an interesting observation considering that both P and N atoms coordinate via the same means – through their lone electron pair.

Although Hermes and Girolami [112] had no interest in the catalytic aspect of their compounds, nor in the mechanisms by which their compounds were formed (i.e. through possible dimeric intermediates), they were able to isolate a crystal structure with the dippe ligand and the analogous titanium precursor $[TiCl_3(thf)_3]$. They found the structure to be dimeric–$[TiCl_3(dippe)]_2$. As in this study, they were unable to isolate the corresponding chromium dimer and made no reference to a dimeric intermediate resulting in the formation of their monomer (i.e. they were suggesting the straightforward substitution of the thf molecules).

$$[CrCl_3(thf)_3] + dippe = [CrCl_3(dippe)(thf)] + 2\ thf$$

During the course of this study, while attempting to synthesise $[CrCl_3(dppe)(pyphenyl)]$ **(22)**, crystals large enough for the diffractometer were obtained. Once solved, it was interesting to find that the compound $[Hpyphenyl][CrCl_4(dppe)]$ **(23)** had formed. This was not completely unexpected as similar structures were obtained for both the pyridine and bipyridine classes of compound. Indeed, this result was once again a strong indication that dimeric intermediates do in fact exist within these systems and provide a plausible route for this and the N–ligand structures.

4.3 SYNTHETIC ROUTE TO PRODUCT FORMATION

The question of whether the precipitates of all the compounds formed within this class came from monomeric or dimeric intermediates was then posed.

Of particular interest was whether, like the monodentate and bidentate N–classes of ligands, there was vibrational evidence to suggest straightforward monomeric substitution of dppe with one remaining thf to give $[CrCl_3(dppe)(thf)]$ **(18)** or would the dimeric species form. Furthermore, would the addition of the respective secondary monodentate para-substituted pyridine derivatives yield the monomeric compounds via direct ligand substitution or symmetrical cleavage of the dimeric intermediate, or would this addition cause asymmetrical cleavage as seen by $[Hpyphenyl][CrCl_4(dppe)]$? A further reason for pursuing the various possible coordination pathways was the fact that the IR of the precipitate obtained from the reaction of $[CrCl_3(thf)_3]$, dppe and pyphenyl was different from that of the crystals of the same reaction. Figure 4.1 provides a summary of the routes to product formation.

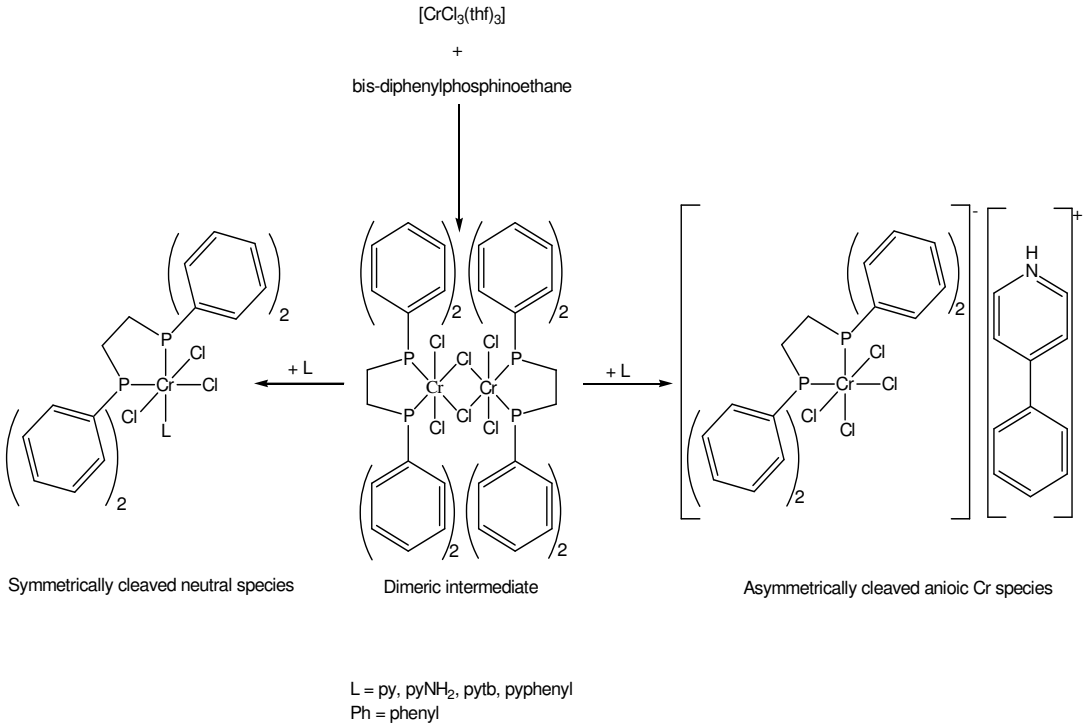

Figure 4.1 **Proposed routes to complex formation**

4.4 INFRARED AND RAMAN SPECTROSCOPY

Considering the obvious difficulty in obtaining single crystals of these compounds, spectroscopic techniques have proved extremely insightful as tools for characterising these compounds. In-depth IR (both MIR and FIR) and Raman analysis of these novel dppe–type compounds provides valuable information regarding coordination, structure, etc. – in particular when the analysis is complemented by the data from the other techniques used in this study.

As is widely recognised, a strong indication of the substitution of thf and subsequent coordination of dppe and the various pyridine derivatives to the metal centre is the shifting of free ligand vibrations to higher frequencies. The band assignments and the respective shifts will now be discussed.

As has been mentioned in connection with the analysis of the other classes of compound, the ability to obtain at least one single-crystal structure of a class of compounds and in turn to analyse the crystal's vibrational data has added a great deal to the confidence with which the vibrational assignments of all compounds within the class have been made. Note that no Raman spectra of either [$CrCl_3$(dppe)(pyphenyl)]

or [Hpyphenyl][$CrCl_4$(dppe)] were obtained as a result of sample fluorescence in the former and insufficient sample of the single-crystal material in the latter.

4.4.1 Region 3313–2863 cm^{-1}

Within this particular region there are a number of vibrations that are common to all the compounds. These include weak bands assigned to overtones that coincide with other metal–dppe complexes [113.]. They range from 3179 to 3130 cm^{-1} in the IR spectrum and from 3172 to 3142 cm^{-1} in the Raman spectrum. Although some of these modes are not visible in the IR, those that are appear at slightly stronger intensities than their Raman counterparts.

C–H bands pertaining to the phenyl (dppe) and heterocyclic (pyridine) rings were also observed in the complexes and can be equally assigned to either ring system as there is sufficient precedence in the literature for both [73, 74**,** 113]. They are present as two vibrations at ~3076 and ~3055 cm^{-1}. That being said, as there is no pyridine present in [$CrCl_3$(dppe)(thf)], its bands at 3076 cm^{-1} (weak in IR spectrum and absent in Raman spectrum) and 3055 cm^{-1} (medium in IR spectrum and strong in Raman spectrum) are related to phenyl C–H [113]. When compared with the corresponding free dppe vibrations, the bands appear to have shifted by 10 and 8 cm^{-1} respectively, which infers coordination. Although the pyridine-based complexes possess C–H vibrations at frequencies very similar to those of [$CrCl_3$(dppe)(thf)], it is nonetheless tempting to assign them all to phenyl C–Hs. This certainly does not imply the absence of pyridine C–Hs, but rather the dominance of phenyl C–Hs in this region. Figure 4.2 highlights the IR band shifts in [$CrCl_3$(dppe)(thf)] relative to free dppe.

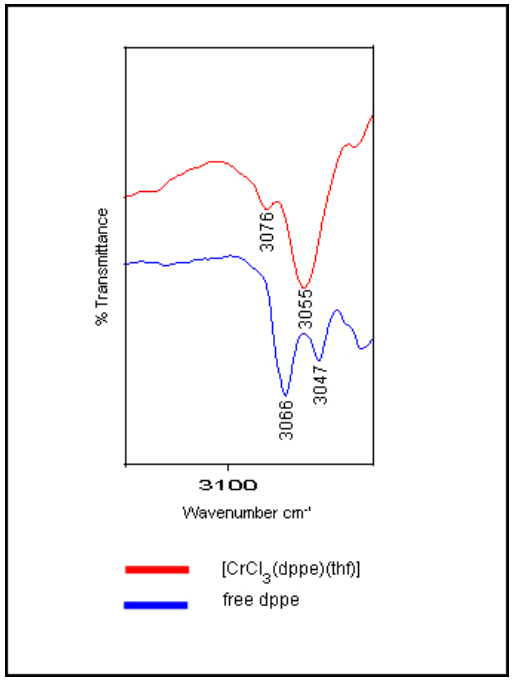

Figure 4.2 **IR spectra showing band shifts in [$CrCl_3$(dppe)(thf)] (red) relative to free dppe (blue)**

Pyridine-specific C–H modes are, however, observed in the IR spectra of [$CrCl_3$(dppe)(py)] **(19)** at 3101 cm^{-1} (shifted from 3083 cm^{-1} in the free ligand) [73, 74] and [$CrCl_3$(dppe)($pyNH_2$)] **(20)** at 3092 cm^{-1} (unshifted as expected) [96].

CH_2 modes that bridge the PP atoms of dppe are also common to more than half of the compounds. Both the CH_2 asymmetrical and symmetrical stretches are visible at ~2956 and ~2925 cm^{-1}, and both are considered to be weak vibrations, particularly in the IR spectra. However, as can be seen from the spectrum of free dppe in Figure 4.3, the mode at ~2926 cm^{-1} is considerably more prominent.

The fact that the band at ~2956 cm^{-1} is of very weak intensity proved to be advantageous when studying the spectrum of [$CrCl_3$(dppe)(pytb)] **(21)** as no ambiguity surrounds the strong vibration at 2964 cm^{-1}. It can therefore be confidently assigned to a CH_3 asymmetrical stretching mode [92, 113] and is shown in Figure 4.3. A close look at the figure also shows that the CH_2 symmetrical stretch at ~2925 cm^{-1} may be observed as a shoulder that has shifted to 2934 cm^{-1} in the complex.

Two other vibrations were observed solely in the spectrum of $[CrCl_3(dppe)(pytb)]$ at 2904 cm^{-1}(medium intensity) IR, 2908 cm^{-1}(medium intensity) Raman and 2869 cm^{-1} (medium intensity) IR, 2868 cm^{-1}(medium shoulder) Raman. They are duly assigned to CH_3 symmetrical stretches. Their minimal degree of shifting relative to the free pytb ligand corresponds to that of other metal–pytb complexes in the literature [92].

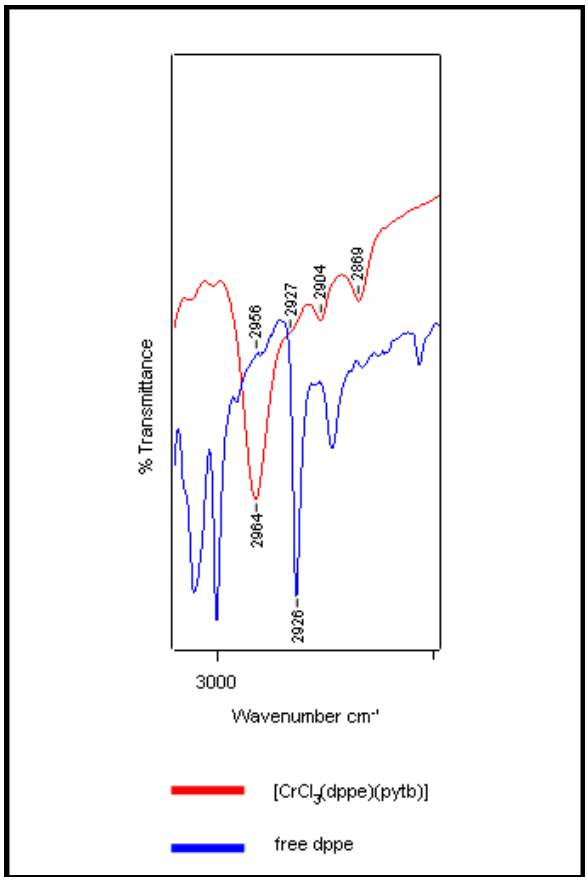

Figure 4.3 **IR spectra of $[CrCl_3(dppe)(pytb)]$ (red) and free dppe (blue)**

Other pyridine substituent bands that are assignable are those associated with the N–H vibrations of the $pyNH_2$ ligand and these are not subject to any ambiguity brought about by the overlap of other ligand vibrations. They are observed as strong IR vibrations at 3313 and 3206 cm^{-1} as highlighted in Figure 4.4, with only the latter visible as a weak vibration in the corresponding Raman spectrum [96].

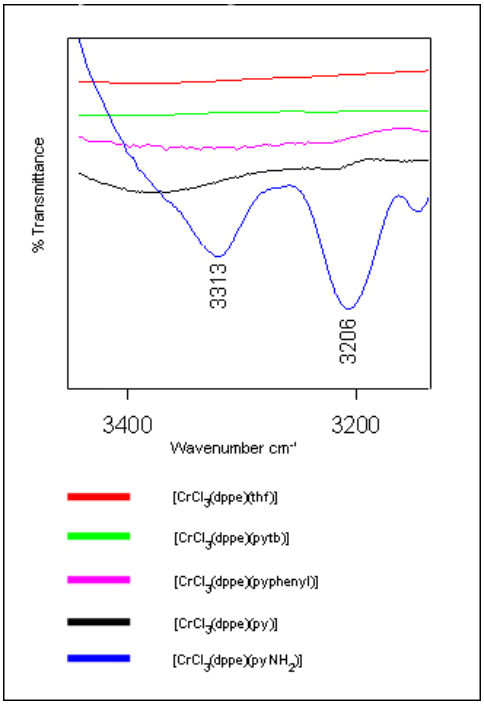

Figure 4.4 **N–H vibrations observed in the IR spectrum of [$CrCl_3$(dppe)($pyNH_2$)] (blue)**

As observed in the previous bipyridine ligand class of compounds, the presence and indeed absence of bands pertaining to the C–H vibrations of thf offer valuable insights into the mechanistic routes leading to compound formation. This essentially centres on the initial reaction involving the addition of dppe to [$CrCl_3(thf)_3$], whereby the presence of C–H thfs indicates direct monomeric ligand substitution, while their absence is indicative of dimeric formation. Unfortunately, the analysis is not as clear-cut as one had hoped owing to band superposition with dppe vibrations, coupled with the broad, shoulder-type nature of the bands in [$CrCl_3$(dppe)(thf)] in the IR spectrum (slightly more prominent in the Raman spectrum). However, as these modes are also present in the spectrum of [Hpyphenyl][$CrCl_4$(dppe)] which is known not to possess coordinated thf, one assumes that the thf modes are absent in [$CrCl_3$(dppe)(thf)]. See Figure 4.5. This is an early indication of dimer formation as opposed to the directly substituted monomeric species that is plausible for the bipyridine equivalent. Although seen to a greater extent in the following region, there is evidence to suggest that this dimeric species can be cleaved both symmetrically and asymmetrically as the compound [Hpyphenyl][$CrCl_4$(dppe)] possesses a strong characteristic pyridinium vibration (asymmetrical cleavage) at 3191 cm^{-1} [94] that is absent in the other complexes (symmetrical cleavage).

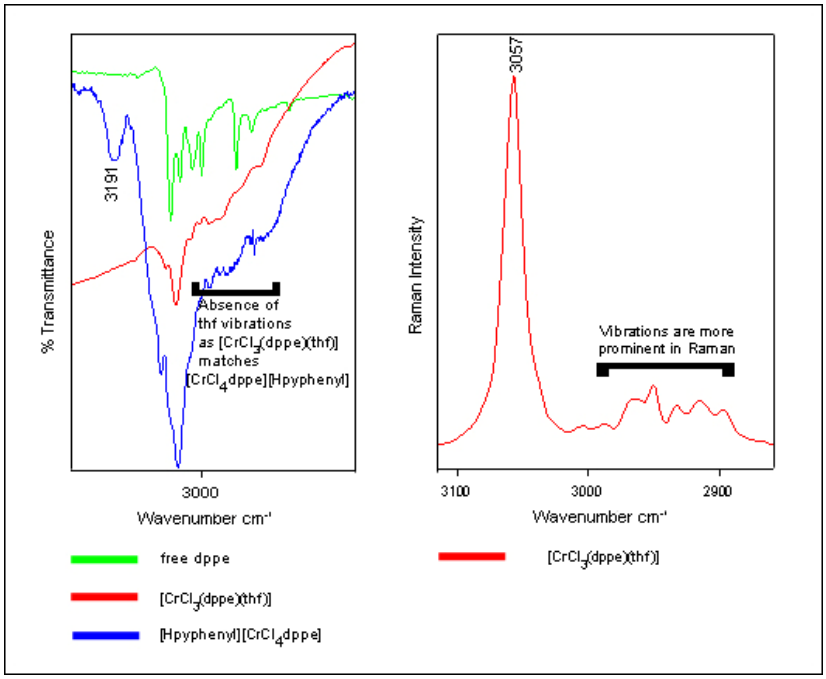

Figure 4.5 **Comparisons between IR spectra of [$CrCl_3$(dppe)(thf)] (red), [Hpyphenyl][$CrCl_4$(dppe)] (blue) and free dppe (green). Raman spectrum of [$CrCl_3$(dppe)(thf)]**

4.4.2 Region 1651 to 1045 cm^{-1}

This is an important region in the assignment of pyridinium vibrations, as well as giving indications of coordination (i.e. characteristic shifts).

The band at ~1632 cm^{-1} is a significant vibration. It is present as a medium to weak vibration in the compounds [$CrCl_3$(dppe)(py)], [$CrCl_3$(dppe)(pytb)] and [$CrCl_3$(dppe)(pyphenyl)], and as a very strong vibration in [Hpyphenyl][$CrCl_4$(dppe)]. Its absence in [$CrCl_3$(dppe)($pyNH_2$)] is more than likely due to it being masked by the strong, broad 1651 cm^{-1} vibration associated with N–H stretching [96]. It is assigned as a ring vibrational mode of pyridine [73, 74], which is reiterated by its absence in [$CrCl_3$(dppe)(thf)]. However, the intensity difference between [Hpyphenyl][$CrCl_4$(dppe)] and the others may be of importance as one cannot rule out the possibility that it is in fact an in-plane ring deformation of the pyridinium ion. This is characterised by a strong IR vibration at 1630 cm^{-1} as opposed to the weaker band that is indicative of pyridine [93].

Another band whose strength may very well be indicative of its assignment is that found between 1617 and 1605 cm^{-1} in all the complexes. Its presence as a medium to

strong vibration (particularly in the IR spectra) in the pyridine compounds correlates well to the shifting of free pyridine vibrations from ~1580 cm^{-1} upon coordination [73, 74]. Although also present in $[CrCl_3(dppe)(thf)]$ and $[Hpyphenyl][CrCl_4(dppe)]$, the vibration is notably weaker and can be assigned to C=C ring stretch of the phenyl ring [92,113].

A representative IR spectrum is shown in Figure 4.6 which highlights the differences in band intensity with respect to the vibrations at ~1630 and 1617 to 1605 cm^{-1} by comparing $[Hpyphenyl][CrCl_4(dppe)]$ and $[CrCl_3(dppe)(py)]$.

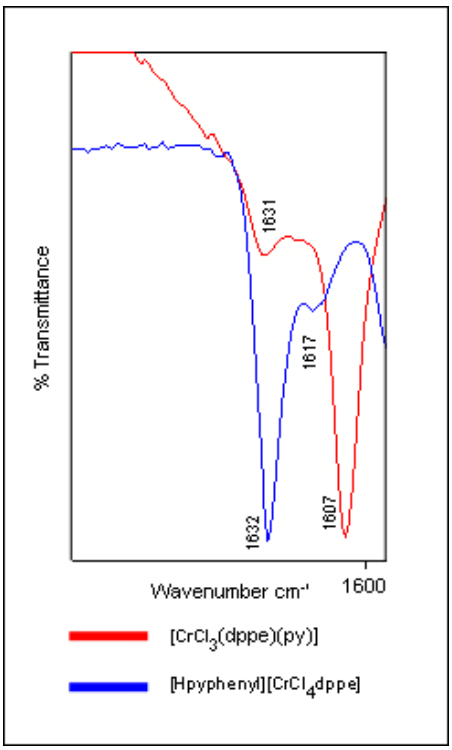

Figure 4.6 **Band intensity comparison between the IR spectra of $[CrCl_3(dppe)(py)]$ (red) and $[Hpyphenyl][CrCl_4(dppe)]$ (blue)**

Referring again to the topic of pyridinium vibrations, three further bands are observed only in $[Hpyphenyl][CrCl_4(dppe)]$ and are therefore assumed to be pyridinium-related. They include two medium-intensity bands at 1515 and 1212 cm^{-1}, as well as two weaker bands at 1495 and 1262 cm^{-1}. The literature proposes a number of other vibrations that are pyridinium-related, including 1530, 1480, 1327, 1250 and 1237 cm^{-1} [93, 94]. Unfortunately, these also coincide with dppe and pyridine vibrations and thus any definitive assignment either way is ambiguous.

With regard to C=C ring vibrations, one is able to assign the band at ~1587 cm^{-1} specifically to dppe C=C [92, 113] and that at ~1535 cm^{-1} to pyridine C=C [73, 74]. This is possible as the former in pyridine has shifted to the higher frequency upon coordination (already discussed), while the latter is absent in both free dppe and $[CrCl_3(dppe)(thf)]$. The only other C=C vibration is found at ~1574 cm^{-1} but is equally assignable to both aromatic systems.

Bands associated with the pyridine substituents are also visible in this region, with those expected to shift upon coordination doing so. The band at 1651 cm^{-1}, as mentioned previously, is identified as a characteristic N–H vibration from the $[CrCl_3(dppe)(pyNH_2)]$ compound that has shifted from 1645 cm^{-1} in the free ligand. There is also a weak C–NH_2 mode observed only in $[CrCl_3(dppe)(pyNH_2)]$ at 1258 cm^{-1} in the IR spectrum and at 1260 cm^{-1} in the Raman spectrum[96].

Bands indicative of the tertiary butyl group of $[CrCl_3(dppe)(pytb)]$ are also visible (Figure 4.7) and are assigned with relative confidence as they do not fall at frequencies where there is a possibility of overlap with other vibrations. Their coordinative shifts correlate well with those in the literature and are as shown in Table 4.1.

Table 4.1 pytb-specific vibrations

Free pytb / cm^{-1}		**$[CrCl_3(dppe)(pytb)]$ / cm^{-1}**		**Shift / cm^{-1}**	
IR	**RAMAN**	**IR**	**RAMAN**	**IR**	**RAMAN**
1494	1495	1500	1503	6	8
1457	1452	1462	1462	5	10

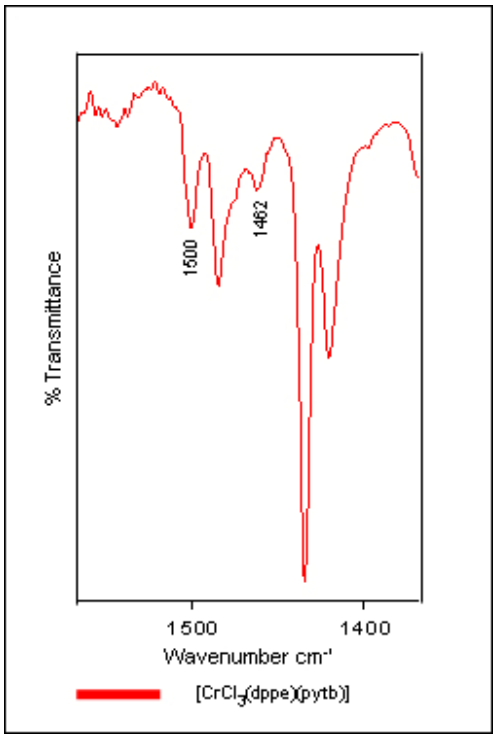

Figure 4.7 IR spectrum of [$CrCl_3$(dppe)(pytb)]-specific vibrations

As one might expect, the phenyl-specific vibrations associated with the pyphenyl ligand in [$CrCl_3$(dppe)(pyphenyl)] are equally assignable to dppe or pyridine ring vibrations.

The remaining bands in this region consist largely of C–H deformations (dppe) and C–H ring stretches (pyridines), with the majority remaining unshifted as is expected.

4.4.3 Region 1026– 519 cm^{-1}

As discussed in Chapters 2 and 3, and well documented in the literature, the band at 992 cm^{-1} in free unsubstituted pyridine shifts to 1015 cm^{-1} upon coordination to the metal centre in the IR spectrum. For the substituted pyridine compounds, the extent of this shift differs depends on the mass, nature and position of the substituent [75]. Although the dppe ligand possesses a band at a similar position to the expected shifts of the compounds, important assignments can still be made.

What is particularly interesting is that the shifts observed for the various pyridine compounds in this class follow the same trend as those for the monodentate and bidentate N–ligand systems. This takes on further importance when one considers that

crystal structures and subsequent IR spectra of coordinated unsubstituted and pytb compounds were obtained, making comparisons particularly meaningful. The dppe vibrations occur at 1026 and 999 cm^{-1} and, as shown in Figure 4.8 which compares both free dppe and $[CrCl_3(dppe)(thf)]$, they do not shift upon complexation. The same figure also shows the Raman spectrum of $[CrCl_3(dppe)(thf)]$ with both bands present at a strong intensity similar to that of the IR bands.

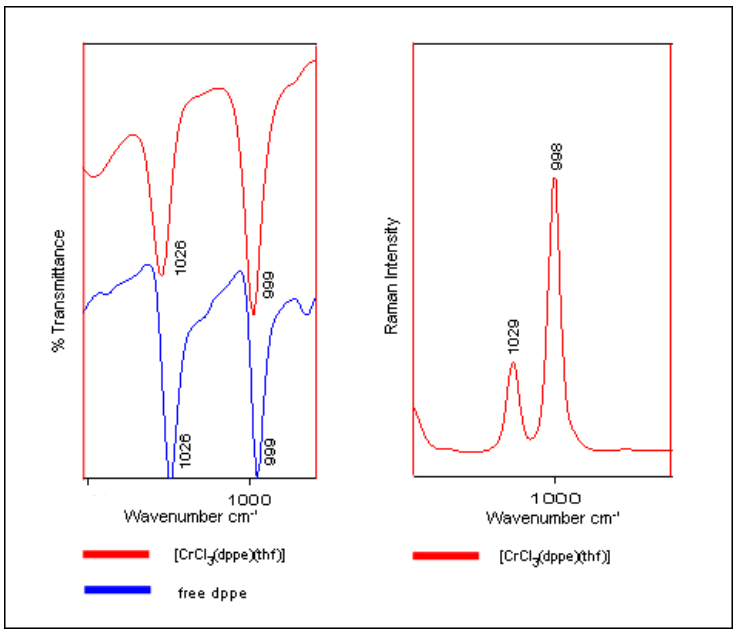

Figure 4.8 **IR and Raman spectra of $[CrCl_3(dppe)(thf)]$ (red) with the IR highlighting the lack of shifting relative to free dppe (blue)**

In $[CrCl_3(dppe)(py)]$ the 992 cm^{-1} band shifts to 1015 cm^{-1} so there is no problem with band overlap, particularly as the band at 1027 cm^{-1} is still visible (Figure 4.9).

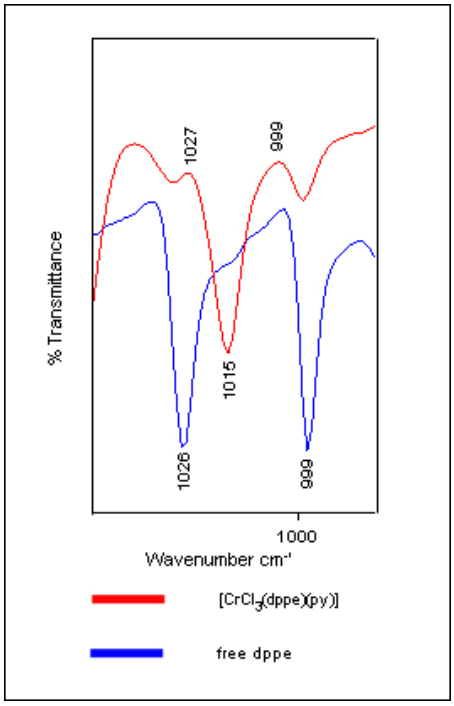

Figure 4.9 **Ring breathing shift in IR bands of [$CrCl_3$(dppe)(py)] (red)**

As expected, the pyNH_2 and pytb compounds, due to their increased mass, show larger shifts and are both found at 1027 cm^{-1}. They are assigned to the pyridine ring breathing shifts as opposed to the free dppe ligand as the free pyridine vibration in both spectra is absent. Therefore it is assumed that the dppe band is masked and not visible. Figure 4.10 shows the IR and Raman spectra.

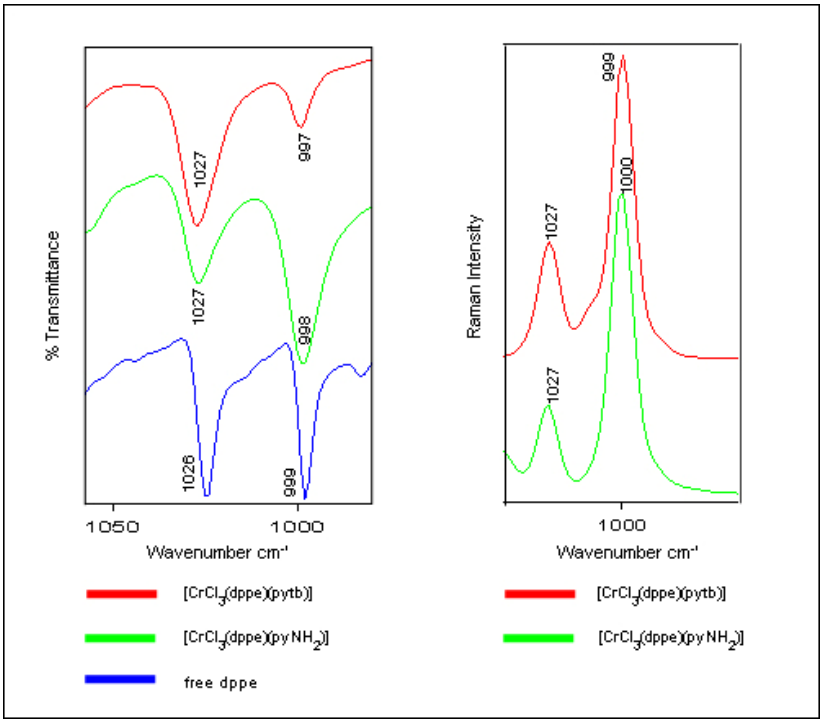

Figure 4.10 IR and Raman spectra of [$CrCl_3$(dppe)($pyNH_2$)] (green) and [$CrCl_3$(dppe)(pytb)] (red)

By following this increasing mass trend, one would expect the pyphenyl compound to show the greatest shift. In the previous N–compounds it was thought that the band at 1026 cm^{-1} was the shifted 992 cm^{-1} band, thus correlating with the expected trend. However, a band at 1011 cm^{-1} was also present and thus a degree of uncertainty arose in assignment. This ambiguity was cleared up by referring to the crystal structure and subsequent IR spectrum of [Hpyphenyl][$CrCl_4$(dppe)]. The band at 1026 cm^{-1} is present and that at 1011 cm^{-1} is absent. This suggests strongly that the 1026 cm^{-1} vibration is not the shifted 992 cm^{-1} band and it is instead assigned to the dppe ligand vibration [113] (Figure 4.11).

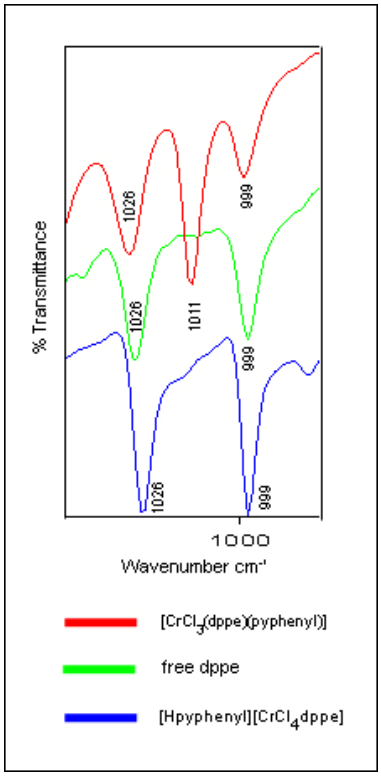

Figure 4.11 **Comparisons between IR spectra of [$CrCl_3$(dppe)(pyphenyl)] (red), [Hpyphenyl][$CrCl_4$(dppe)] (blue) and free dppe (green)**

It would seem that, perhaps somewhat surprisingly, due to its mass it is the 1011 cm^{-1} band that is assigned to the coordinated pyphenyl. Although the trend by mass is not followed, it serves to confirm that mass is not the only factor that determines the degree of shifting (see Table 4.2).

Table 4.2 **Shifting of the characteristic ring breathing vibration in [$CrCl_3$(dppe)(py)], [$CrCl_3$(dppe)($pyNH_2$)], [$CrCl_3$(dppe)(pytb)] and [$CrCl_3$(dppe)(pyphenyl)]**

Pyridine / cm^{-1}	[$CrCl_3$(dppe)(py)] / cm^{-1}	Shift / cm^{-1}
990	1015	25

$pyNH_2$ / cm^{-1}	[$CrCl_3$(dppe)($pyNH_2$)] / cm^{-1}	Shift / cm^{-1}
991	1027	36

Pytb / cm^{-1}	[$CrCl_3$(dppe)(pytb)] / cm^{-1}	Shift / cm^{-1}
995	1027	32

Pyphenyl / cm^{-1}	[$CrCl_3$(dppe)(pyphenyl)] / cm^{-1}	Shift / cm^{-1}
1001	1011	10

This result has further implications with regard to the nature of the products formed as what is implied by the above shifts is that the secondary amine ligands have indeed coordinated to the chromium centre. This results in neutral monomeric species, most probably from the symmetrical cleavage of the dimeric intermediate proposed from the results of region 3313 to 2863 cm^{-1}. The alternative would have been the asymmetrical cleavage of the dimer resulting in pyridinium-type compounds similar in nature to [Hpyphenyl][$CrCl_4$(dppe)] in which this specific pyridine shift is absent.

Yet further evidence of [Hpyphenyl][$CrCl_4$(dppe)] being the only pyH complex is the medium-intensity band at 819 cm^{-1} (see Figure 4.12) which is present only in [Hpyphenyl][$CrCl_4$(dppe)]. It is thus assumed to be associated with pyH.

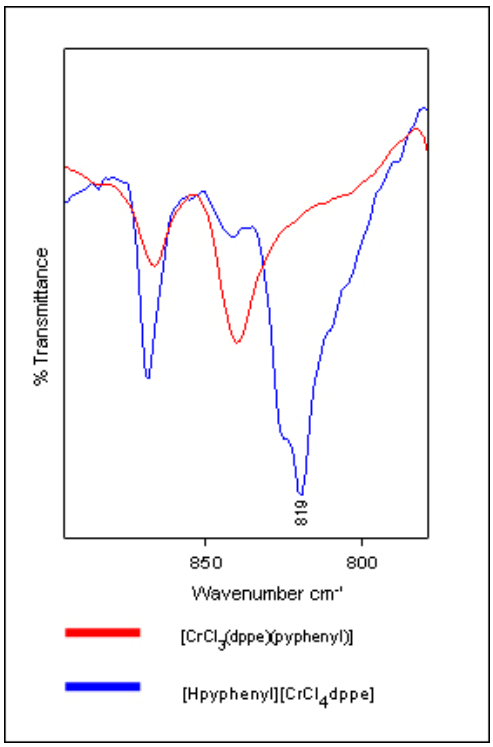

Figure 4.12 **IR spectra showing pyH-specific vibration in [Hpyphenyl][$CrCl_4$(dppe)] (blue) which is absent in [$CrCl_3$(dppe)(pyphenyl)] (red)**

Another pyridine vibration that characteristically shifts upon coordination is observed at 643 cm^{-1} in [$CrCl_3$(dppe)(py)], having shifted from 604 cm^{-1} in its free form [73, 74]. Unlike the shifting of the above-mentioned band at 992 cm^{-1}, this shift is indicative solely of unsubstituted coordinated pyridine, hence its absence in the other compounds.

Another vibration deserves mention as its very presence is indicative of dppe ligand coordination. It is observed at ~654 cm^{-1} in all the complexes and is assigned to P–C stretch of the five–membered chelate ring [113], hence its absence in free dppe.

A representation of the above data from all the compounds is given in Figure 4.13 which compares $[CrCl_3(dppe)(py)]$, $[CrCl_3(dppe)(pytb)]$, $[CrCl_3(dppe)(thf)]$ and free dppe.

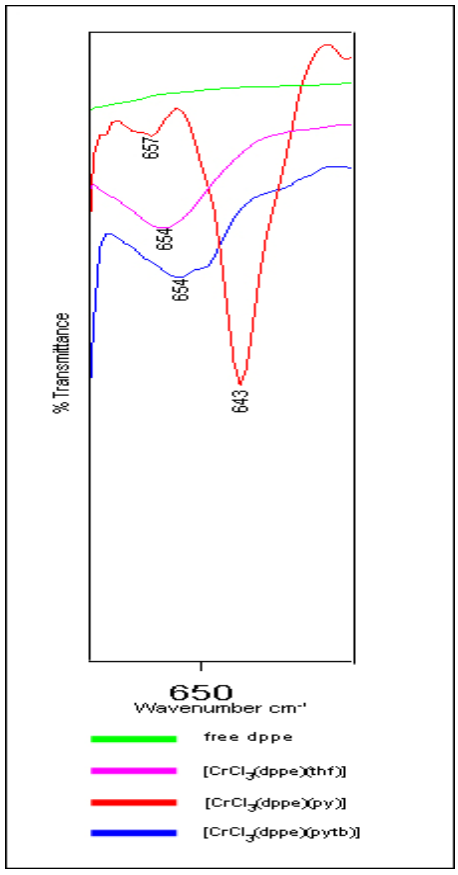

Figure 4.13 IR spectra of $[CrCl_3(dppe)(py)]$ (red), $[CrCl_3(dppe)(pytb)]$ (blue), $[CrCl_3(dppe)(thf)]$ (purple) and free dppe (green)

As expected, there are a considerable number of dppe-related vibrations in this region. Most are unshifted, except for that at 521 cm^{-1} which is indicative of in-plane quadrant ring stretch [113] and has notably shifted from the free ligand position of 505 cm^{-1}.

Within this region the presence of a band at ~856 cm^{-1} is perhaps the strongest indication of coordinated thf (C–O–C) [114]. It is, however, notably absent in the

complexes, including [$CrCl_3$(dppe)(thf)]. This is yet further evidence that this particular complex is the dimeric species as opposed to the directly substituted, monomeric [$CrCl_3$(dppe)(thf)] complex. This finding can be further confirmed by looking at the IR spectrum of a similar compound, [$CrCl_3$(dippe)(thf)], documented in the literature [112]. It has been characterised as a monomeric species and although not discussed as part of this study, its IR spectrum does possess a band at 856 cm^{-1} which in the light of this study confirms its monomeric status.

The remaining vibrations are specific to the pyridine substituent (Table 4.3). The majority pertain to the tertiary butyl group of [$CrCl_3$(dppe)(pytb)] at values that are expected upon coordination [92].

Table 4.3 pytb specific vibrations

Free pytb / cm^{-1}		**[$CrCl_3$(dppe)(pytb)] / cm^{-1}**		**Shift / cm^{-1}**	
IR	**RAMAN**	**IR**	**RAMAN**	**IR**	**RAMAN**
927	931	926	934	-1	3
711	710	729	729	18	19
569	572	571	564	2	-8

Unlike the other regions, there are two additional bands that can be confidently assigned to the phenyl substituent on the pyridine ring of pyphenyl. They are observed in the spectra of [$CrCl_3$(dppe)(pyphenyl)] and [Hpyphenyl][$CrCl_4$(dppe)] only, at ~912 and 625 cm^{-1} respectively, and correlate with the literature, with the latter shifting significantly from the free ligand position of 608 cm^{-1} [97].

4.4.4 Region 495-215 cm^{-1}

In addition to the characteristic metal–ligand vibrations found in this region, there are a further two bands that deserve comment. The first is a well-characterised IR vibration associated with coordinated unsubstituted pyridine at 444 cm^{-1} that has shifted from the free ligand position of 404 cm^{-1} [73, 74]. Note that a very weak vibration is visible at 435 cm^{-1} in the corresponding Raman spectrum.

The second relates to a tertiary butyl C–C–C deformation observed as a weak vibration at 399 cm^{-1} in both the IR and Raman spectra. According to the literature, it has shifted from a free ligand value of 392 cm^{-1} in the IR spectrum [92].

The metal–ligand vibrations of interest include Cr–P, Cr–Cl and Cr–N (py). The band at ~415 cm^{-1} in the spectra of all the complexes is tentatively assigned to a Cr–P vibration as although there is precedence in the literature for such an assignment involving other metals [114, 115], there is also the possibility that it is a dppe vibration shifted from 400 cm^{-1}. In either case it still infers dppe coordination.

In accordance with the IR data of the previous chapters, one expects the presence of three Cr–Cl vibrations between ~390 and ~300 cm^{-1} to be indicative of the *mer* monomer [80]. This is observed for all the pyridine-based complexes for which the IR bands are stronger than their Raman counterparts.

The $[CrCl_3(dppe)(thf)]$ compound deserves closer inspection. Although three weak vibrations are present in the Raman spectrum (indicating monomer), a more complex IR spectrum is observed with what appears to be four vibrations that fall within the so–called 'Cr–Cl range'. It is very difficult to confirm that these vibrations are a direct consequence of the formation of the dimeric species. What is, however, clear is that the vibrational pattern differs from that of all the other complexes in this class which all have strong precedence in the literature for their respective assignments. Importantly, it also differs from the spectrum of $[CrCl_3(dippe)(thf)]$ (two vibrations in this range) which, as stated earlier, was confirmed by Hermes and Girolami [112] to be monomeric (*cis* conformer [80]). Therefore by a process of elimination one of the very few remaining options is a dimeric species.

Another important vibration in the N–classes of compounds was that at 221 cm^{-1} which was confidently assigned to Cr–N (py) [41, 80, 81]. Unfortunately, due to the presence of Ph–P–Ph vibrations from the dppe ligand at a very similar frequency [113], overlap of bands was observed. Assignment was therefore ambiguous.

Figure 4.14 is a representation of the spectra from all the complexes, encompassing all details discussed above. The complexes include [$CrCl_3$(dppe)(thf)], [$CrCl_3$(dppe)(py)] and [$CrCl_3$(dppe)(pytb)].

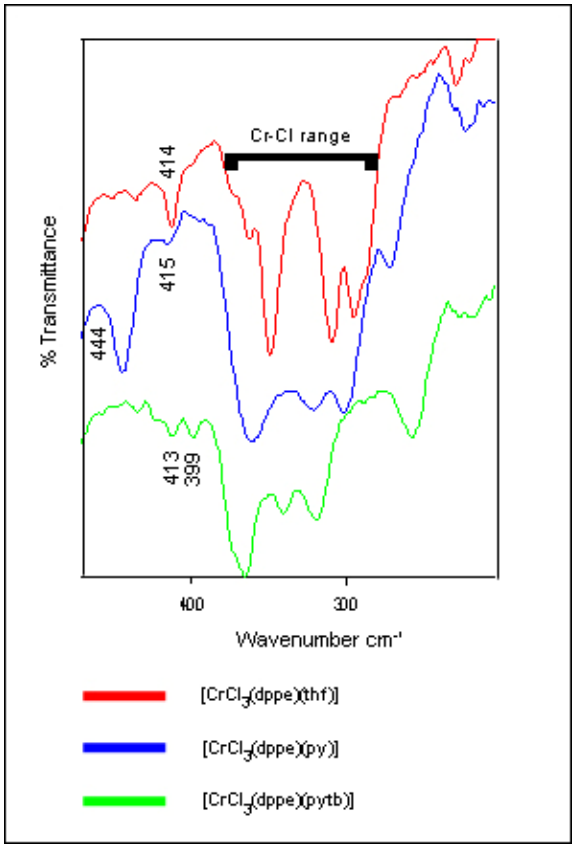

Figure 4.14 **FIR spectra of [$CrCl_3$(dppe)(thf)] (red), [$CrCl_3$(dppe)(py)] (blue) and [$CrCl_3$(dppe)(pytb)] (green)**

Finally, examination of the spectra of [$CrCl_3$(dppe)(pyphenyl)] and [Hpyphenyl][$CrCl_4$(dppe)] importantly confirm that they are not the same complex (Figure 4.15). [$CrCl_3$(dppe)(pyphenyl)] shows the bands indicative of the monomeric species, with two strong vibrations and one that is notably weaker (either way it is either the *cis* or *mer* conformer). [Hpyphenyl][$CrCl_4$(dppe)] possesses three strong vibrations with a further two weaker vibrations.

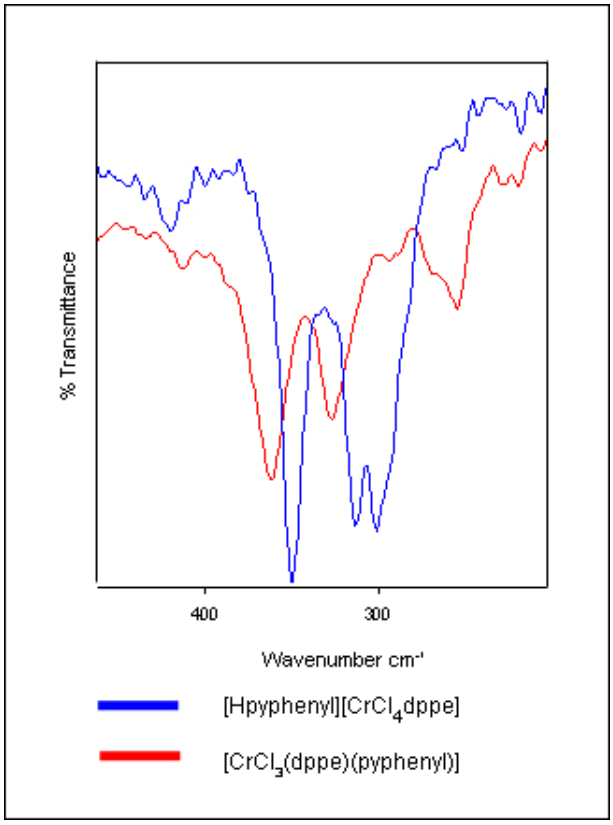

Figure 4.15 **FIR spectra of [$CrCl_3$(dppe)(pyphenyl)] (red) and [Hpyphenyl][$CrCl_4$(dppe)] (blue)**

In conclusion, the detailed vibrational study suggests that the complex initially suggested as [$CrCl_3$(dppe)(thf)], on the basis of the equivalent bipy structure, is [Cr(dppe)Cl_2(μ-Cl)]$_2$. The other compounds in this class show sufficient vibrational evidence to be monomeric in structure.

Table 4.4 **Vibrational assignments of $[CrCl_3(dppe)(thf)]$ (18), $[CrCl_3(dppe)(py)]$ (19), $[CrCl_3(dppe)(pyNH_2)]$ (20), $[CrCl_3(dppe)(pytb)]$ (21), $[CrCl_3(dppe)(pyphenyl)]$ (22) and [Hpyphenyl][$CrCl_4(dppe)$] (23)**

18		19		20		21		22	23	Assignment
IR / cm^{-1}	RAMAN / cm^{-1}	IR / cm^{-1}	RAMAN / cm^{-1}	IR / cm^{-1}	RAMAN / cm^{-1}	IR / cm^{-1}	RAMAN / cm^{-1}	IR / cm^{-1}	IR / cm^{-1}	
-	-	-	-	3313s	-	-	-	-	-	ν(NH_2) asym (76, 96)
-	-	-	-	3206s	3212w	-	-	-	-	ν(NH_2) sym (76, 96)
-	-	-	-	-	-	-	-	-	3191s	pyH
-	3172w	3157w	3167w	-	3169w	-	3169w	-	3179m	Overtone (113)
3141w	3145w	3133w	3140w	3143s	3142w	3141w	3141w	3136w	-	Overtone (113)
-	-	-	-	-	-	3130w	-	-	-	Overtone (113)
-	-	3101s/s	-	-	-	-	-	-	-	ν(CH) (py) (73, 74)
-	-	-	-	3092ssh	3092msh	-	-	-	-	ν(CH) ($pyNH_2$) (96)
3076w	-	-	3079s/s	-	-	3076ssh	3088sh	3076ssh	3086s	ν(CH) (dppe) (113)
3055m	3057s	3062s/s	3051s/s	3055s	3054s	3053s	3051s	3047s	3049s	ν(CH) (dppe) (113) / (py) (73, 74)

18		19		20		21		22	23	Assignment
3003w	3003w	3004ssh	3002w	3009sh	3003w	3003m	3002m	-		Combination (113)
2986m	2987w	-	-	2972s	2982w		-	2972s	2984s	Combination (113)
-	-	-	-	-	-	2964s	2965s	-	-	ν (CH_3) asym (92)
2956sh	2950m	2959w	2957w	-	2957m	-	-	-	2961w 2947w	ν (CH_2) asym (113)
2926sh, 2915sh	2932m, 2915m	2929w	2915w	-	2915m	2934sh	-	-	-	ν (CH_2) sym (113)
-	-	-	-	-	-	2904m	2908m	-	-	ν (CH_3) sym (92)
2878sh	2896m	2892ssh	2891w	-	2890m	-	-	2872s 2833s	2888s 2863s	Present in free dppe (unassigned)
-	-	-	-	-	-	2869m	2868msh	-		ν (CH_3) sym (92)
-	-	-	-	1651vs	1650m	-	-	-	-	δ (NH_2) (96)
-	-	1631m 1607s	1633w 1605m	-	-	1634m 1616s	1636w 1617w	1635w 1612s	1632s 1617w	ν_{ring} (py) (73, 74, 92, 97) / pyH (93, 94)
1617m	1617vw	-	-	-	-	-	-	-	-	unassigned
1587m	1587s	1584brsh	1585s	1587s	1585s	1586w	1585s	-	1590m	ν_{ring} (dppe) (113)

18		19		20		21		22	23	Assignment
1572m	1574m	1571w	1572m	1572sh	1573msh	1572w	1572msh	1568w	1577w	ν_{ring} (dppe) (113) / ν_{ring} (pyX) (73-75, 92, 96, 97)
-	-	1535m	1535vw	1529vs	1534m	1542w	1542vw	1539w	-	ν_{ring} (pyX) (73-75, 92, 96, 97)
-	-	-	-	-	-	-	-	-	1515m	PyH related
-	-	-	-	-	-	1500m	1503vw	-	-	ν_{ring} (pytb) (92)
-	-	-	-	-	-	-	-	-	1495w	PyH related
1485m	1487w	1485s	1487w	1484m	1486w	1485m	1484w	1480s	1482s	CH def + ν(semicircle) (113)
-	-	-	-	-	-	1462w	1462w	-	-	CH_3 asym def (92)
-	-	1445vs	-	-	-	-	-	-	-	ν_{ring} (py) (73, 74)
1435s	1434w	1432s	1437w	1434s	1435w	1434vs	1437m	1432s	1432s	CH def + ν(semicircle) (113)
1416m	1420w	1417w	1417w	1414w	1414w	1420s	1416w	1413m	1417m	Overtone(113) / CH_3 sym def (92) / ν_{ring} (97)

18		19		20		21		22	23	Assignment
-	-	-	-	1362w	-	1365w	-	-	1363m	ν_{ring} (96) / CH_3 asym def (92)
1334w	1337w	1333w	1333w	1336w	1333vw	1332w	1331w	1332w	1334w	δ (CH) def (113)
1314w	1312w	-	-	1314w	1306vw	1308w	1308vw	1310w	-	δ (CH) def (113) / ν_{ring} (pyphenyl) (97)
-	-	-	-	-	-	-	-	1288vw	1286m	ν_{ring} + ν(CH) (pyphenyl) (97)
1270w	1274w	1268w	1272w	1271w	1271w	1274m	1273w	-	-	CH_2 wag (113)
-	-	-	-	-	-	-	-	-	1262w	PyH related
-	-	-	-	1258w	1260w	-	-	-	-	ν (C-NH_2) (96)
-	-	1236w 1220m	- 1224w	1214w	-	1230m	1233w	1222m	1237w	ν_{ring} (73-75, 92, 96, 97)
-	-	-	-	-	-	-	-	-	1212m	PyH related
1190w 1160w	1195m 1163m	1196w 1155m	1197m 1158m	1197m 1158w	1194m 1159m	1190m 1157m	1191m 1159m	1188w 1155w	1189m 1156w	δ (CH) def (113)
1120wsh	1116msh	-	-	-	-	1121sh	1124w	-	-	ν (P-(C_6H_5)) (113)
1099m	1110m	1110m	1099m	1098m	1099m	1098s	1098m	1096m	1098m	Ring breathing (113)
1071w	1076vw	1069s	1073vw	1072w	-	1069s	1070m	1067m	1068m	δ (CH) def (113)

18		19		20		21		22	23	Assignment
-	-	1046m	1046w	1056w	1046m	-	-	1045m	-	ν_{ring} (73-75, 96, 97)
1026w	1029s	1027w	1028sh	-	-	-	-	1026m	1026m	δ (CH) def (113)
-	-	1015m	1018s	1027m	1027s	1027s	1027s	1011m	-	Ring breathing (pyX) (73, 74, 92, 96, 97)
999w	998vs	999w	998s	998m	1000s	997m	999s	999m	997m	Trigonal ring breathing (dppe) (113)
-	-	-	-	-	-	926w	934w	-	-	CH_3 rock (tb) (92)
-	-	-	-	-	-	-		912w	913w	ν (CH) pyphenyl (97)
868w	872w	864w	-	864w	-	867m	868vw	864m	868w	i.p o.p. def (113) / CH_3 rock (tb) (92) / CH py (73, 74, 92, 96, 97)
-	-	-	-	847sh	849s	843sh	842w	838m	841w	X-sens (96) / py breathing (92) / ν_{ring} (97)
827w	835w	823w	825w	825m	831sh	832s	827w	-	-	In phase γ(CH) def (113, 96, 92)
-	-	-	-	-	-	-	-	-	819m	PyH related

18		19		20		21		22	23	Assignment
-	-	758s	766w	-	765w	-	764w	764s	761s	γ(CH) (py) (73-75, 92, 96, 97)
741s	741vw	746s	746vw	742s	746vw	742s	-	742s	748s	In phase γ(CH) (dppe) (113)
-	-	-	-	-	-	-	-	-	737s	In phase γ(CH) (dppe) (113)
-	-	-	-	-	-	729m	729m	-	-	γ(CH) (pytb) (92)
-	-	-	-	-	-	-	-	-	708s	PyH related
693s	698m	694vs	700wsh	695s	-	691vs	-	691s	690s	CH_2 rock (113)
-	684m	679m	685m	-	683m	-	686m	-	-	γ (sextant ring) def (113)
-	-	-	-	-	-	668m	668m	-	-	ν (CC) (pytb) (92)
-	-	-	-	-	-	-	-	-	663w	PyH related
654w	665w	657vw	650w	645w	647m	653w	651w	654w	656m	ν (PC) (5-membered ring) (113)
-	-	-	-	-	-	-	-	-	648w	PyH related
-	-	643s	637w	-	-	-	-	-	-	ν_{ring} (py) (73, 74)
-	-	-	-	-	-	-	-	625m	626vw	Pyphenyl vib
613w	617m	616vw	617m	616w	617m	617w	617m	617w	617w	δ (quadrant ring) def (113)

18		19		20		21		22	23	Assignment
-	-	-	-	-	-	571m	564vw	-	-	Skeletal str (tb) (92)
-	-	-	-	-	-	-	-	-	550w	PyH related
-	-	-	-	-	-	546m	548vw	-	-	Rock (tb) (92)
521s	524m	520s	521w	525s	527m	522s	520w	523s	519s	δ (quadrant ring) def (113) / X-sens $pyNH_2$ (96)
495m	490vw	490sh	488vw	495s	491vw	494m	488vw	492s	497m 488m	δ (quadrant ring) def (113)
475sh	469vw	476m	473vw	-	475vw	474sh	474vw	-	-	unassigned
-	-	444m	435vw	-	-	-	-	-	-	ν_{ring} (py) (73, 74)
414m	413m	415w	-	413m	412m	413w	417w	413w	420w	Cr –P (114, 115)
-	-	-	-	-	-	399w	399w	-	-	CCC def (pytb) (92)
363m	370w	361m	367w	375w	370w	365m	367w	361s	349s	Cr – Cl (80)
									334w	Cr – Cl (80)
349m	344w	321m	341w	348m	337w	340m	336w	326s	326w	Cr – Cl (80)
308m	306w	301m	324w	309m	309w	319m	316w	293w	312s	Cr – Cl (80)
294m	-	-	-	-	-	-	-	-	300s	Cr – Cl (80)

18		19		20		21		22	23	Assignment
227w 220w	- 221w	229w 219w	222w 217w	222w 215w	227w -	226w 216w	228m -	225w 218w	224vw 216vw	Ph – P – Ph (113) Cr – N (py) (41, 80, 81)

ν = stretching, δ = in-plane bending, γ = out-of-plane bending, def = deformation, asym = asymmetrical, sym = symmetrical vs = very strong, s = strong, m= medium, w = weak, vw = very weak

4.5 COMPUTATIONAL STUDY

Computational analysis was carried out solely on [$CrCl_3$(dppe)(pytb)] on the basis of it being a sound representative model of all the complexes. Figures 4.16 and 4.17 illustrate the goodness of fit between the experimental MIR and Raman spectra and their respective calculated spectra. Unlike the analogous studies in the previous chapters, the FIR spectral comparison is also given (Figure 4.18) as this is the first compound of this study in which the solid-state effects do not hinder the observance of all three distinct Cr–Cl vibrations in the calculated spectrum. However, as one has now come to expect with these types of complex, the calculated vibrations are not pure Cr–Cl vibrations but are mixed with other modes.

These vibrations, along with a selection of other important frequencies, are presented in Tables 4.5 which show the excellent correlation and are thus further evidence to support the experimental deductions pertaining to ligand coordination.

At this stage, if any discrepancies in correlation have been observed, they have been associated largely with the metal–ligand vibrations. Therefore it was particularly satisfying to be able to confirm the Cr–P vibration by way of experimental–calculated correlations as it was initially a rather tentative assignment in the experimental analysis.

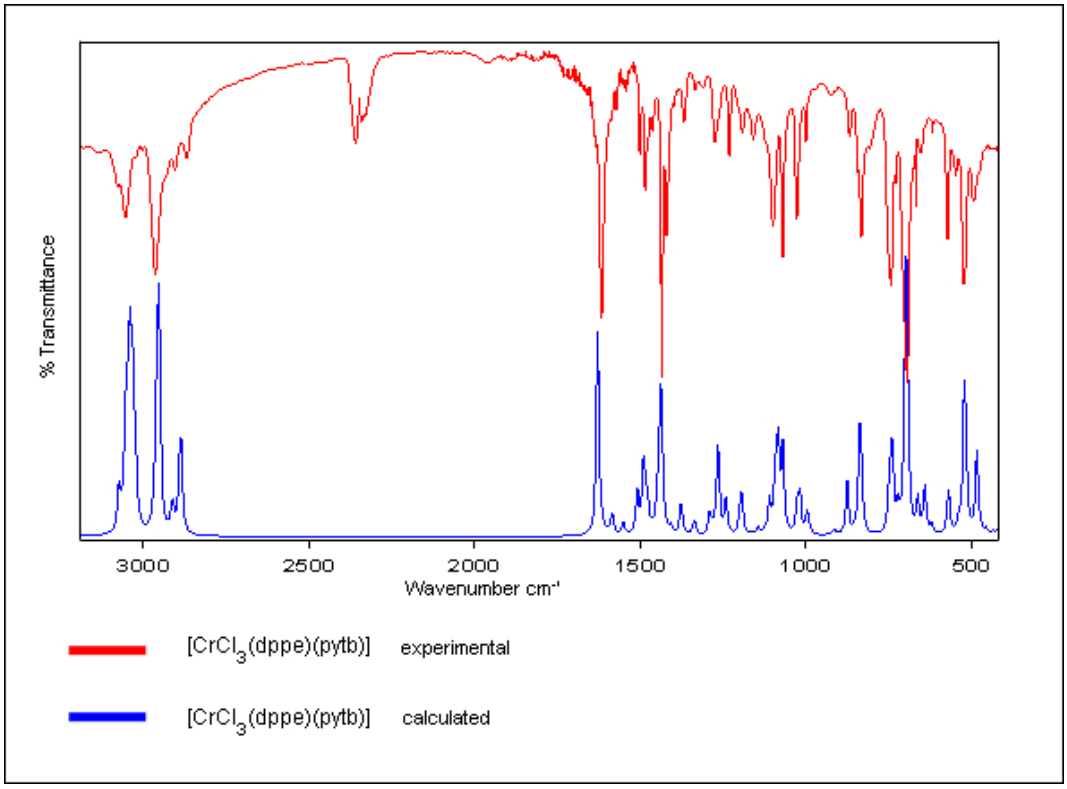

Figure 4.16 **Experimental (red) and calculated (blue) MIR spectra of [$CrCl_3$(dppe)(pytb)]**

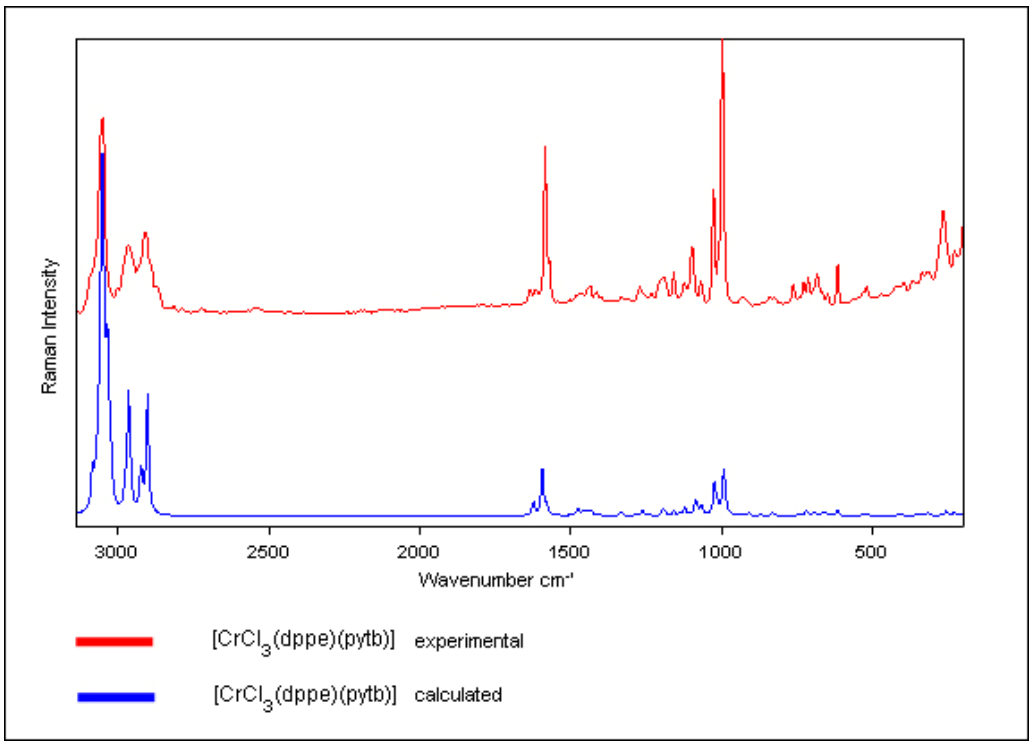

Figure 4.17 **Experimental (red) and calculated (blue) Raman spectra of [$CrCl_3$(dppe)(pytb)]**

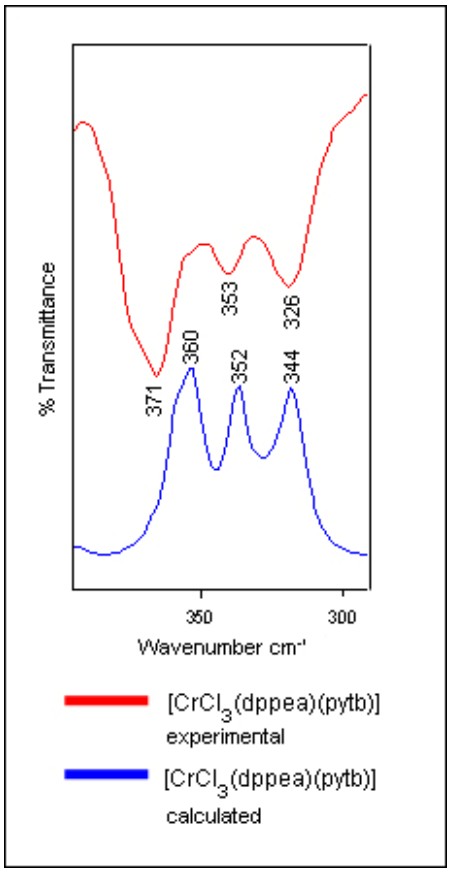

Figure 4.18 **Experimental (red) and calculated (blue) FIR spectra of [$CrCl_3$(dppe)(pytb)]**

Table 4.5 **Selected experimental and calculated IR and Raman band assignments for [$CrCl_3$(dppe)(pytb)]**

[$CrCl_3$(dppe)(pytb)] IR / cm^{-1}		[$CrCl_3$(dppe)(pytb)] Raman / cm^{-1}		Assignment	
Experimental	**Calculated**	**Experimental**	**Calculated**	**Experimental**	**Calculated**
2964	2957	2965	2967	$\nu(CH_3)$ asym	$\nu(CH_3)$ asym
2904	2891	2908	2901	$\nu(CH_3)$ sym	$\nu(CH_3)$ sym
1616	1628	1617	1624	ν_{ring} (py)	ν_{ring} (py)
1586	1585	1585	1596	ν_{ring} (dppe)	ν_{ring} (dppe)
1027	1023	1027	1021	Ring breathing (pytb)	Ring breathing (pytb)

997	997	999	995	Trigonal ring breathing (dppe)	Trigonal ring breathing (dppe)
653	660	651	660	ν (PC) (5-membered ring)	ν (PC) (5-membered ring)
413	416, 408	417	416, 407	Cr–P	Cr–P
365, 340, 319	358, 336, 317	367, 336, 316	358, 336, 318	Cr–Cl	Cr–Cl + tb breathing / tb rock / CH_3 twist
226, 219	240	228	239	Ph–P–Ph / Cr–N (py)	Cr–N (py)
-	232	-	232		Ph–P–Ph

Table 4.6 Scaling factors determined for [$CrCl_3$(dppe)(pytb)]

Region / cm^{-1}	IR	Raman
0 – 1861	0.980144	0.978311
2827 – 3424	0.953311	0.956743

The generation of the molecular orbitals associated with [$CrCl_3$(dppe)(pytb)] allows one to see that both the HOMO and LUMO orbitals are found around the chlorine atoms (Figure 4.19). Where differences arise is in the phenyl ring systems, where electrophilic attack is likely to take place on those rings that are found on the P–Cr–N axis, while attack by nucleophilic species will take place on the rings on the Cl–Cr–P axis.

HOMO **LUMO**

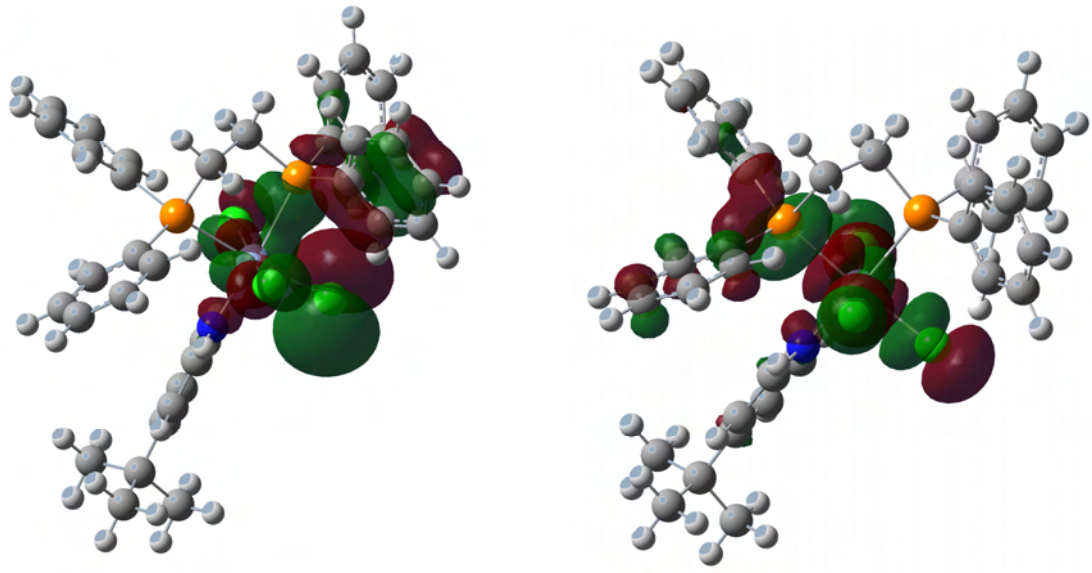

Figure 4.19 HOMO and LUMO orbitals of [$CrCl_3$(dppe)(pytb)]

4.6 NMR SPECTROSCOPY

As a result of the lack of aromaticity or conjugation associated directly with the coordinating phosphorus atoms, the substitution reaction resulting from the addition of dppe to [$CrCl_3(thf)_3$] was not followed by ^{1}H NMR spectroscopy as dppe ligand resonances were not expected to disappear upon coordination to the metal centre.

This was confirmed when the spectrum of the final product (see Figure 4.20) was recorded in DMSO-d_6 in which the aromatic protons are observed at 7.3 ppm and the CH_2 protons at 2.01 ppm.

On the basis of the deductions made in Chapter 3, the notable absence of thf resonances may suggest that this is a dimeric species, which would correlate with the deductions made in the corresponding IR and Raman spectral interpretation.

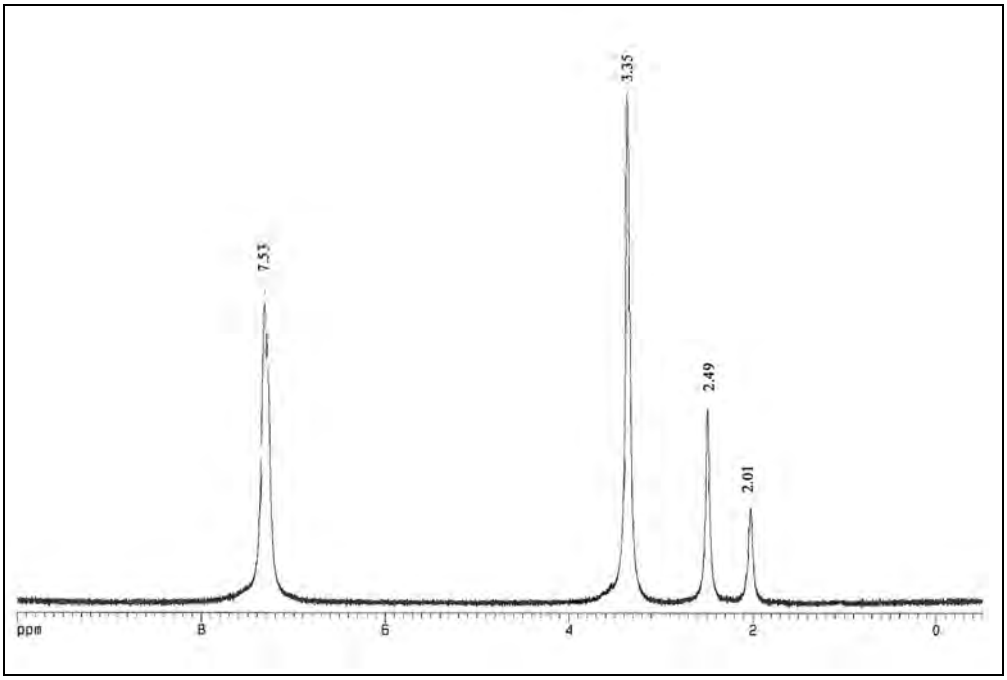

Figure 4.20 **^{1}H NMR spectrum of [$CrCl_3$(dppe)(thf)] final product in DMSO-d_6**

The presence of phosphorus in the ligand allowed ^{31}P NMR spectroscopy to be used. Spectra of both the free ligand and the [$CrCl_3(thf)_3$] plus dppe compound were recorded and a clear resonance shift of 5.25 ppm was observed upon coordination (Figures 4.21 and 4.22).

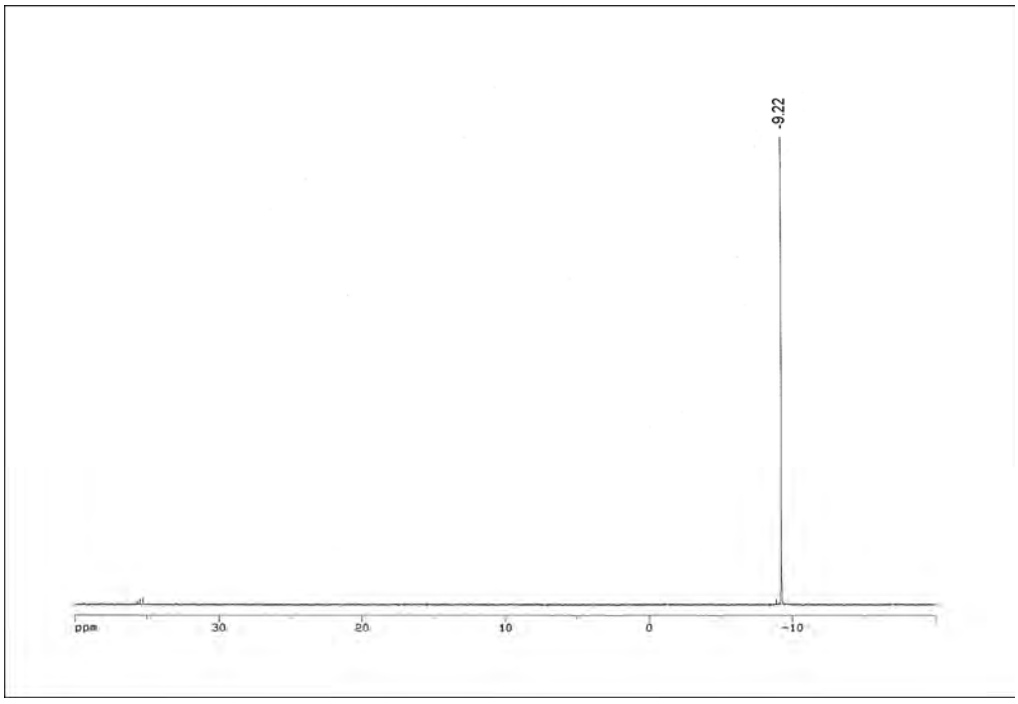

Figure 4.21 **^{31}P NMR spectrum of free dppe in DMSO-d_6**

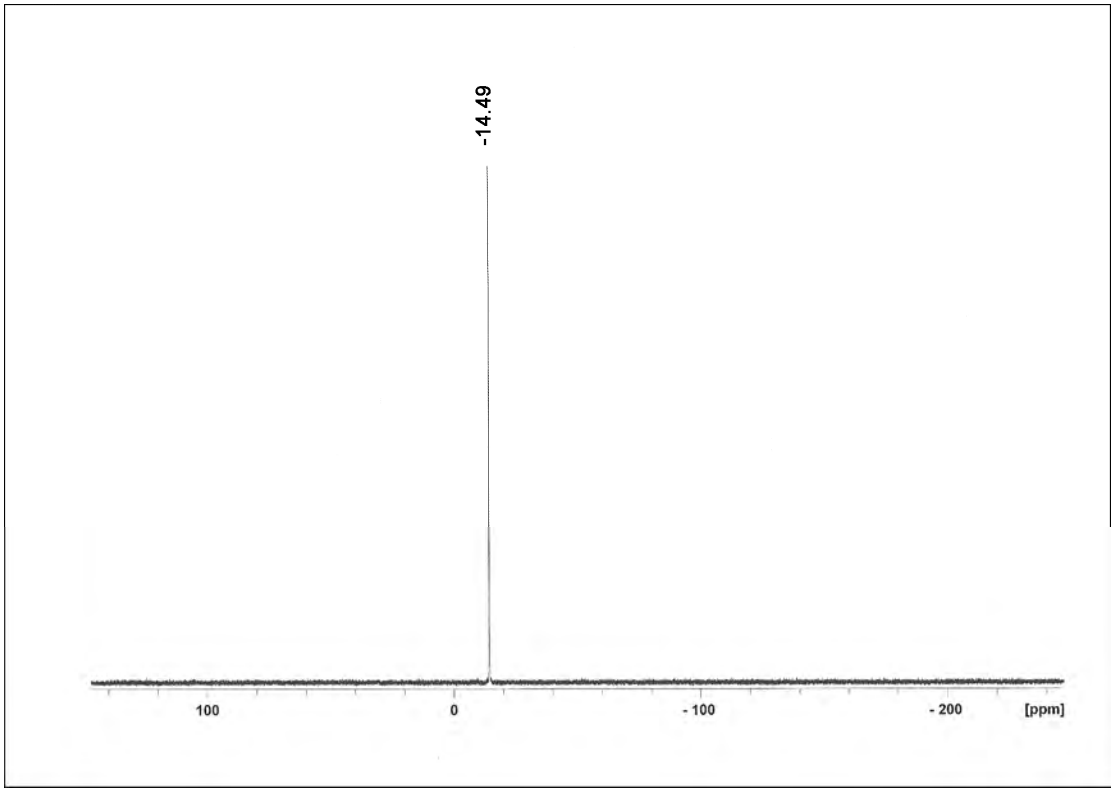

Figure 4.22 **^{31}P NMR spectrum of [$CrCl_3$(dppe)(thf)] in DMSO-d_6**

4.7 MASS SPECTROMETRY

As with the previous classes a selection of compounds were chosen for analysis. These included [$CrCl_3$(dppe)(thf)], [$CrCl_3$(dppe)($pyNH_2$)] and [$CrCl_3$(dppe)(pyphenyl)]. All three compounds showed good isotopic distribution patterns for the fragment that resulted from the loss of the respective monodentate ligands and a chlorine atom, i.e. $[M–thfCl]^+$, $[M–pyNH_2Cl]^+$ and $[M–pyphenylCl]^+$ (m/z = 520). This same fragment without a further chlorine atom was also observed for each of the compounds with similarly good distribution patterns ($[M–thf2Cl]^+$, $[M–pyNH_22Cl]^+$ and $[M–pyphenyl2Cl]^+$) (m/z = 485). These results are presented in Figure 4.23 The spectrum of [$CrCl_3$(dppe)(pyphenyl)] shown in Figure 4.24 also possessed an additional fragmentation pattern, $[M–Cl]^+$ (m/z = 675), which confirms its monomeric structure. Note that all of the above mentioned isotopic distribution patterns correlated well with those determined theoretically. It is plausible that the distribution patterns observed for [$CrCl_3$(dppe)(thf)] and [$CrCl_3$(dppe)($pyNH_2$)] could be fragments of a dimeric species. For the former compound this correlates well with the vibrational data, while the latter's vibrational spectra suggest the monomer. This structural deduction for [$CrCl_3$(dppe)($pyNH_2$)] is also based on the compound's

similarity to [$CrCl_3$(dppe)(pyphenyl)] in terms of the addition of a monodentate substituted pyridine ligand which yielded strong MS evidence for the monomer.

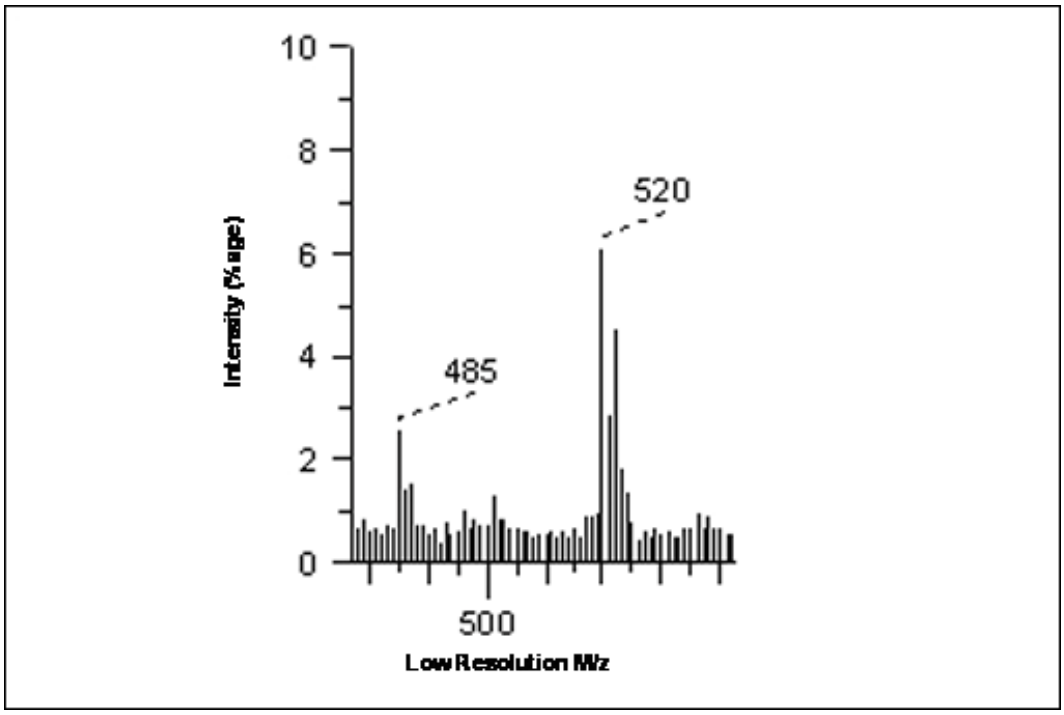

Figure 4.23 FAB-MS spectum showing paeks present in [$CrCl_3$(dppe)(thf)], [$CrCl_3$(dppe)($pyNH_2$)] and [$CrCl_3$(dppe)(pyphenyl)]

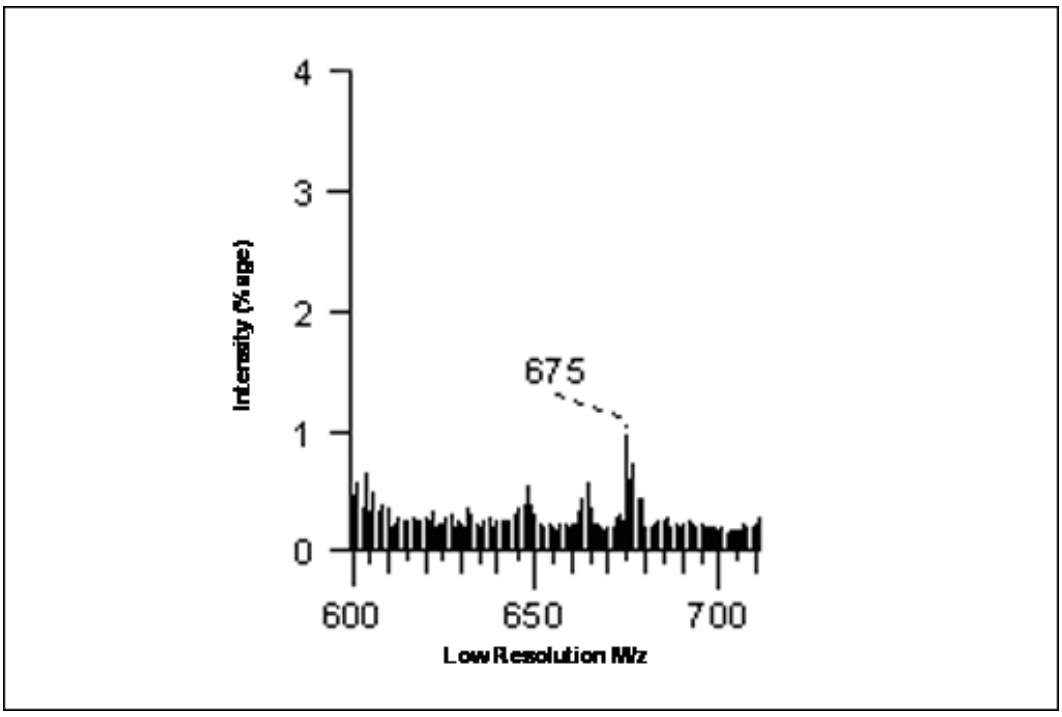

Figure 4.24 FAB-MS spectrum of [$CrCl_3$(dppe)(pyphenyl)]

4.8 X-RAY CRYSTALLOGRAPHY

4.8.1 [Hpyphenyl][$CrCl_4$(dppe)]

The molecular structure of [Hpyphenyl][$CrCl_4$(dppe)] is the only structure of a diphenylphosphinoethane–tetrachloro–chromium complex anion. Although the coordination geometry is similar to that of the tetra–n–propylammonium (*cis*–1,2–bis(diphenylphosphino) ethylene tetrachloro chromium(III) structure determined by Gray [99], there are significant structural differences arising from the reduction of the 'CC bridge' bond order, as well as from the novel counter-ion interactions that are absent in the 'Gray structure'.

Two formula units are observed in the asymmetrical unit of [Hpyphenyl][$CrCl_4$(dppe)] (Figure 4.25) as opposed to one formula unit in the Gray structure. The chromium atom is coordinated to four chlorine atoms and the two phosphorus atoms of the dppe ligand. The coordination is approximately octahedral, with the largest angle deviation being the P(3)–Cr(2)–Cl(8) (81.76(8)°). All other *cis* X–Cr–Y bond angles in the two formula units are in the range 81.93(7) to 96.27(8)°. These values are comparable to those found for the Gray structure.

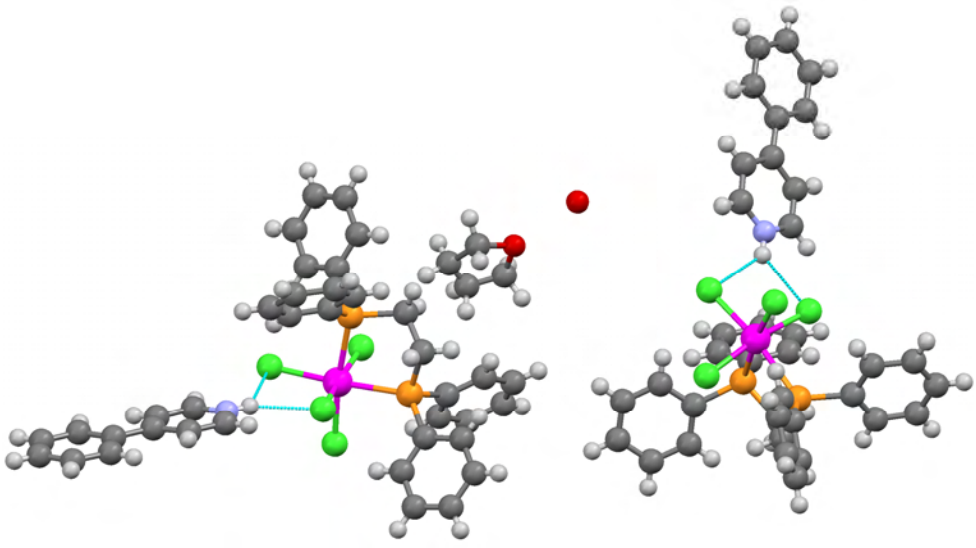

Figure 4.25 **Perspective drawing of the asymmetric unit of [Hpyphenyl][$CrCl_4$(dppe)] showing hydrogen bond interactions**

The metal–ligand bond lengths were also found to be very similar in the two structures (Table 4.7). The similarities continue with regard to both crystal system and space group as both crystallised in a triclinic space group, P–1.

The same cannot be said for the torsion angle comparisons. A large twist is observed for the P–C–C–P torsion angle of this study's structure (61.2(6)°) as opposed to the corresponding angle in the Gray structure, which twists 4.12° in the opposite direction. This feature makes any comparisons between the two structures' magnitudes of phenyl ring twisting awkward as there is no fixed P–C reference common to both structures. Suffice it to say that Figure 4.26 clearly shows that there are notable differences between the two.

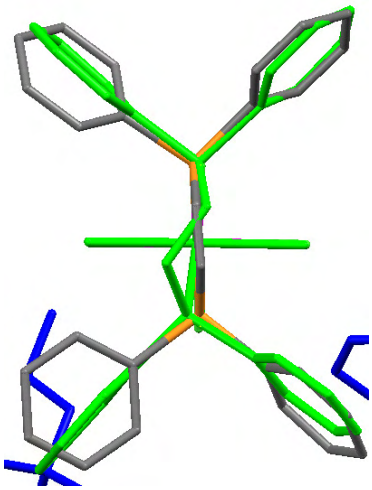

Figure 4.26 **P–C–C–P torsion angle comparison between [Hpyphenyl][$CrCl_4$(dppe)] and the Gray structure**

Table 4.7 **Bond lengths [Å] and angles [°] for [Hpyphenyl][$CrCl_4$(dppe)]**

Cr(1)-Cl(4)	2.310(2)	Cr(1)-Cl(2)	2.3450(19)
Cr(1)-Cl(3)	2.319(2)	Cr(1)-P(2)	2.492(2)
Cr(1)-Cl(1)	2.3401(19)	Cr(1)-P(1)	2.494(2)
Cl(4)-Cr(1)-Cl(1)	94.54(7)	Cl(8)-Cr(2)-Cl(6)	94.03(8)
Cl(3)-Cr(1)-Cl(1)	91.88(7)	Cl(6)-Cr(2)-Cl(7)	91.38(8)
Cl(4)-Cr(1)-Cl(2)	93.96(7)	Cl(8)-Cr(2)-Cl(5)	93.70(8)
Cl(3)-Cr(1)-Cl(2)	93.87(7)	Cl(6)-Cr(2)-Cl(5)	96.27(8)

Cl(1)-Cr(1)-Cl(2)	94.17(7)	Cl(7)-Cr(2)-Cl(5)	92.63(8)
Cl(4)-Cr(1)-P(2)	83.19(7)	Cl(8)-Cr(2)-P(3)	81.76(8)
Cl(3)-Cr(1)-P(2)	88.22(7)	Cl(6)-Cr(2)-P(3)	92.70(8)
Cl(1)-Cr(1)-P(2)	92.52(7)	Cl(7)-Cr(2)-P(3)	91.03(7)
Cl(4)-Cr(1)-P(1)	88.20(7)	Cl(8)-Cr(2)-P(4)	89.00(8)
Cl(3)-Cr(1)-P(1)	84.57(7)	Cl(7)-Cr(2)-P(4)	84.96(8)
Cl(2)-Cr(1)-P(1)	91.53(7)	Cl(5)-Cr(2)-P(4)	89.13(8)
P(2)-Cr(1)-P(1)	81.93(7)	P(3)-Cr(2)-P(4)	82.16(7)

P(1)-C(1)-C(2)-P(2)	59.8(7)	P(3)-C(3)-C(4)-P(4)	-61.2(6)
C(1)-P(1)-C(11)-C(12)	20.3(8)	C(3)-P(3)-C(71)-C(76)	33.6(8)
C(1)-P(1)-C(11)-C(16)	-164.6(6)	C(3)-P(3)-C(71)-C(72)	-145.8(7)
C(1)-P(1)-C(21)-C(26)	138.3(7)	C(3)-P(3)-C(81)-C(82)	178.2(7)
C(1)-P(1)-C(21)-C(22)	-46.8(8)	C(3)-P(3)-C(81)-C(86)	-5.2(9)
C(2)-P(2)-C(31)-C(32)	-171.2(6)	C(4)-P(4)-C(91)-C(92)	133.3(6)
C(2)-P(2)-C(31)-C(36)	11.5(7)	C(4)-P(4)-C(91)-C(96)	-47.8(7)
C(2)-P(2)-C(41)-C(42)	145.2(7)	C(4)-P(4)-C(101)-C(106)	157.1(6)
C(2)-P(2)-C(41)-C(46)	-36.3(9)	C(4)-P(4)-C(101)-C(102)	-22.7(7)

Although absent in the Gray structure, hydrogen bonding is present between the pyridinium N–H and the two closest chlorine atoms which are *cis* to each other Table 4.8). This is observed in both formula units in which N(1)–H(1) is hydrogen bonded to Cl(1) and Cl(3) and N(2)–H(2) is hydrogen bonded to Cl(5) and Cl(7). Figure 4.25 above illustrates the hydrogen bonding in one of the two formula units that are present in the asymmetrical unit.

Table 4.8 Hydrogen bonds for [Hpyphenyl][$CrCl_4$(dppe)] [Å and °]

D-H...A	d(D-H)	d(H...A)	d(D...A)	<(DHA)
N(1)-H(1)...Cl(1)	0.86	2.62	3.255(7)	131.9
N(1)-H(1)...Cl(3)	0.86	2.44	3.183(6)	145.1
N(2)-H(2)...Cl(5)	0.86	2.55	3.217(10)	134.8

N(2)-H(2)...Cl(7)	0.86	2.62	3.330(9)	140.0

The lattice packing of the structure is shown in Figure 4.27 and the crystal data in Table 4.9.

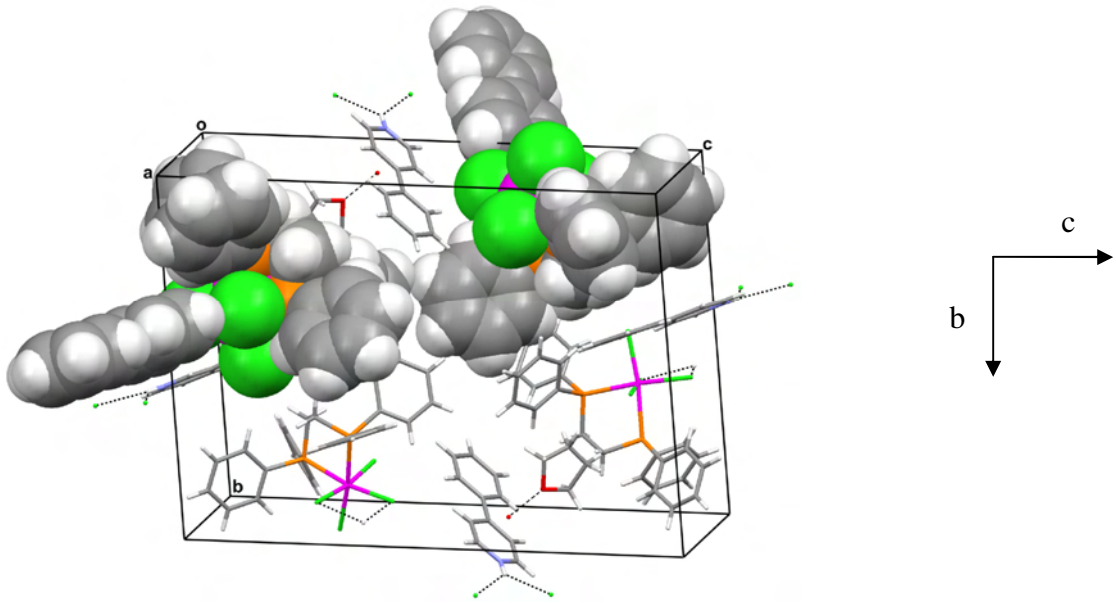

Figure 4.27 **Packing arrangement with space-filled component of [Hpyphenyl][$CrCl_4$(dppe)]**

Table 4.9 **Crystal data and structure refinement for [Hpyphenyl][$CrCl_4$(dppe)]**

Empirical formula	$C_{38.14}$ $H_{36.28}$ Cl_4 Cr N $O_{0.42}$ P_2	
Formula weight	771.10	
Temperature	293(2) K	
Wavelength	0.71073 Å	
Crystal system	Triclinic	
Space group	P 1	
Unit cell dimensions	a = 10.3411(16) Å	α= 86.581(3)°
	b = 16.328(3) Å	β= 85.538(3)°
	c = 22.859(3) Å	γ = 89.934(2)°
Volume	3 841.2(10) $Å^3$	
Z	4	
Density (calculated)	1.333 Mg/m^3	

Absorption coefficient	0.688 mm^{-1}
F(000)	1 590
Crystal size	0.22 x 0.08 x 0.08 mm^3
Theta range for data collection	2.56 to 26.53°
Index ranges	-12<=h<=11, -19<=k<=18, -28<=l<=11
Reflections collected	20 512
Independent reflections	13639 [R(int) = 0.0613]
Completeness to theta = 25.00°	96.7%
Absorption correction	Semi-empirical from equivalents
Max. and min. transmission	0.946 and 0.855
Refinement method	Full-matrix least-squares on F^2
Data / restraints / parameters	13 639 / 0 / 836
Goodness-of-fit on F^2	1.002
Final R indices [I>2σ(I)]	R1 = 0.0733, wR2 = 0.1836
R indices (all data)	R1 = 0.1599, wR2 = 0.2364
Extinction coefficient	0
Largest diff. peak and hole	0.819 and -0.669 e.$Å^{-3}$

4.9 EXPERIMENTAL

4.9.1 SYNTHESIS OF [$CrCl_3$(dppe)(thf)] / [Cr(dppe)Cl_2(μ-Cl)]$_2$ (18)

A Schlenk tube was charged with [$CrCl_3(thf)_3$] (0.28 g, 0.747 mmol) and thf (20 cm^3). The resulting dissolved purple solution turned a deep blue colour immediately upon addition of dppe (0.29 g, 0.747 mmol). The reaction was then allowed to stir at room temperature overnight to ensure completion. The volume of the final solution was then reduced, followed by the addition of Et_2O (20 cm^3), resulting in the formation of a light blue precipitate. The deep blue supernatant was removed via syringe and the residue dried under reduced pressure for 3 hours, which resulted in the isolation of a light blue precipitate **(18)** in good yield (monomer: 0.41 g, 87% / dimer: 0.41 g, 50%).

4.9.2 SYNTHESIS OF [$CrCl_3$(dppe)(py)] (19)

A Schlenk tube was charged with [$CrCl_3(thf)_3$] (0.31 g, 0.827 mmol) and thf (20 cm^3). Upon dissolution, dppe (0.33 g, 0.827 mmol) was added and the deep blue solution allowed to stir for a period of 10 minutes. At this point pyridine (0.06 cm^3, 0.827 mmol) was added, which afforded an immediate colour change to a blue-green solution. This reaction mixture was left to stir overnight at room temperature. Following the reduction of the final reaction solution, Et_2O (20 cm^3) addition allowed the formation a blue-green residue. After removal of the supernatant via syringe, the residue was washed with Et_2O (20 cm^3) and then allowed to dry under reduced pressure. The resulting precipitate **(19)** was present in good yield (0.41 g, 79%).

4.9.3 SYNTHESIS OF [$CrCl_3$(dppe)($pyNH_2$)] (20)

A Schlenk tube was charged with [$CrCl_3(thf)_3$] (0.27 g, 0.721 mmol) and thf (20 cm^3), followed 3 minutes later by the addition of dppe (0.28 g, 0.721 mmol) to yield a deep blue solution. Following a stirring period of ~10 minutes, $pyNH_2$ (0.06 g, 0.721 mmol) was added, yielding a lighter coloured supernatant coupled with a blue precipitate. To ensure completion the reaction mixture was stirred at room temperature overnight. The precipitate was then washed with Et_2O (20 cm^3) and dried under reduced pressure to afford a light blue precipitate **(20)** in good yield (0.33 g, 75%).

4.9.4 SYNTHESIS OF [$CrCl_3$(dppe)(pytb)] (21)

A Schlenk tube was charged with [$CrCl_3(thf)_3$] (0.30 g, 0.801 mmol) and thf (20 cm^3). Following the addition of dppe (0.32 g, 0.801 mmol), the ligand pytb (0.1 g, 0.801 mmol) was added to yield a blue-green reaction solution that was left to stir at room temperature overnight. The subsequent reduction of the solution, followed by the addition of Et_2O (20 cm^3), led to the formation of a blue-green precipitate. After removal of the supernatant via syringe, the residue was dried under reduced pressure for a period of 3 hours, which resulted in the isolation of a blue-green precipitate **(21)** in good yield (0.47 g, 85%).

4.9.5 SYNTHESIS OF [$CrCl_3$(dppe)(pyphenyl)] (22)

A Schlenk tube was charged with [$CrCl_3(thf)_3$] (0.27 g, 0.721 mmol) and thf (20 cm^3). Upon dissolution, dppe (0.28 g, 0.721 mmol) was added, followed 10 minutes later by pyphenyl (0.11 g, 0.721 mmol). The rich royal blue solution was stirred overnight at room temperature, followed by reduction and Et_2O (20 cm^3) addition to yield a blue-green precipitate. Removal of the supernatant via syringe and drying of the sample under reduced pressure for 3 hours allowed the isolation of a blue-green precipitate **(22)** in good yield (0.46 g, 90%).

Crystals of [Hpyphenyl][$CrCl_4$(dppe)] **(23)** were obtained from the rich royal blue reaction solution after a period of 3 weeks.